doi: 10.1255/tosf.125

High-resolution PAT monitoring of sample preparation grinding by accelerometer sensors: the key to ensuring accuracy and long-term consistency


Martin Lischka


André Mehling

Martin Lischka and André Mehling
HERZOG Maschinenfabrik GmbH & Co. KG, Germany

Industrial operations are often based on critical quality measures obtained for technical process control and/or to determine the value of raw materials and product streams. Process Analytical Technology (PAT) monitoring is applied to characterise, for example, raw materials, semi-finished as well as finished products. There is an active interest in approaches for "smart" online, real-time industrial sensor applications, especially where industrial operations involve high sample throughput and/or may involve hazardous substances demanding *automation*. State-of-the-art sample preparation procedures and equipment can deliver key performances indicators, often supplemented by sensor data that are used as *proxy* quality measures which helps to ensure measurement representativity and optimal process/product control. We here illustrate this industrial front-line arena by an example in which PAT accelerometer data are used for real-time monitoring of the efficiency of the automated grinding sample preprocessing process.

Introduction

Process Analytical Technologies (PAT) has seen an enormous application rush in the last 20 years, starting out in pharma and chemical industries, and has recently seen many creative applications also in industrial sectors well beyond this origin.[1] Various PAT sensor methods and approaches have been developed for specific purposes within the industrial automation realm, e.g. to monitor torque in spear sampling systems, to ensure constant material feeds and also for monitoring milling machines that treat metal samples. Here parameters representing the physical phenomena *vibration* and *torque* are used to monitor the condition of cutting tips of active milling heads. For example, if tool cutting tips are not in the right condition, correct removal of sample surface layers cannot be assured with subsequent adverse analytical results.[2]

Background

Mineral raw materials are often pressed as fine powder (typically less than 75 µm) into steel rings and analysed with X-ray fluorescence (XRF). The calibration of the analytical device is linked to a certain target particle size distribution as manifested by the calibration standards used. For optimal analytical quality this particle size distribution needs to be in compliance for all subsequent routine samples in the longest possible post-calibration period of routine application. However, there is often a lack of methods to monitor compliance for long enough periods in order to ensure the necessary analytical accuracy and constancy.

Disc mills are used in the automated laboratory to comminute granular sample material by grinding, typically reducing the grain size from 1–5 mm down to 150 µm, and below. The eccentric movement of grinding vessels puts the internal grinding set (puck and ring) into circular motion. The sample particles are ground due to shearing, impacting and compression of the material between the grinding set elements and the wall of the vessel. In many instances, the ground material is subsequently pelletised and analysed, e.g. by XRF. The grain size distribution following grinding has a significant impact on the quality of the XRF results. The so-called *particle size effect* may cause variances in elemental analysis of more than 30 % only due to different particle size distribution and

Figure 1. Examples of sample preparation equipment for pressed pellet preparation used in automated XRF analysis. A: Various grinding and pressing accessories for manual sample preparation setup. B: Grinding vessel with sample material. C: Finished pressed pellet suitable for XRF analysis. D: Mill and press combination (HP-MP) used in automatic sample preparation for XRF analysis.

not to compositional differences between samples.[2] It is, therefore, critical to minimise the variability of grain size distribution after grinding in order to decrease this sample preparation bias of the analytical results.

For many materials, the reproducibility of grain size distribution after grinding is very high. This is especially true because of the use of automatic pulverising mills compared to equipment with more manual sub-process stages involved. For other materials and applications, post-grinding grain size distributions may exhibit a higher (to distinctly high) degree of variability due to variation in material constitution. In the automated laboratory realm, it is practically impossible to determine particle size distribution *after* each grinding run. It would consequently be of great help if the grinding efficiency could be monitored in real time *during* the grinding process.

Here, we show that the start and duration of the grinding process can be easily identified from simple acceleration monitoring data. We first provide insights that acceleration signals correlate well with grinding efficiency and with grain size distribution. Based on comparative results from initial experiments we are able to elucidate the underlying mechanism for diagnostic changes in acceleration-monitored milling signals. Routine monitoring based on acceleration data functions as satisfactory proxies for the contemporary grain size distribution, allowing significantly better process monitoring and control.

Comparative study

All tests reported here were carried out on i) a manually loaded grinding vessel [HSM 100P, tungsten carbide (TC)], ii) semi-automatic chrome steel vessel (HP-M 500) or iii) a fully automatic disc mill (model HP-MP, TC vessel). In each case, an acceleration sensor was mounted on the lower half of the swinging aggregate and connected to the programmable logic controller of the grinding mill for data acquisition. For analysis of the grinding vessel motion, the acceleration in both x- and y-directions was assessed. For evaluation of grinding efficiency, the root mean squares (RMS) of the x- and y-accelerations were calculated as previously described,[3,4] allowing RMS levels to be plotted over time for graphic evaluation. We also calculate the standard deviation (SD) of the individual RMS values to determine the ensemble RMS variability.

In some instances, we also analysed the grain size distribution of the ground material using a vibratory sieve shaker.

Results

Acceleration signals representing an empty grinding vessel: efficient and inefficient grinding

For this initial test series, we used the HSM 100P disc mill. First, we assessed acceleration during motion of an empty grinding vessel without sample material (only puck and ring) at a rotation speed of 1000 rpm. Second, we performed a grinding run with 50 g of pure silica sand at a grinding speed of 1000 rpm, resulting in a significant grain size reduction (efficient grinding), and, third, 50 g of the same material was ground at a lower speed of 600 rpm leading to only minor grain size reduction (inefficient grinding). The duration of each grinding run was identical, 30 s.

The empty grinding vessel (Figure 2A) is characterised by a very uniform signal without fluctuations over time. The mean RMS was 30.1 $m s^{-2}$, the mean SD of the ensemble RMS was low at 1.4. During efficient grinding (Figure 2B), the initial acceleration signal was relatively constant with a low variability (RMS 29.9 ± 2.8 $m s^{-2}$). After 8.5 s, however, (red arrow in Figure 2B), there was a significant change in the signal pattern with a constant increase of the variability (RMS 31.3 ± 5.1 $m s^{-2}$). During inefficient grinding (Figure 2C), the acceleration signal remained unchanged with little variability throughout the entire grinding period (RMS 11.8 ± 1.2 $m s^{-2}$).

Influence of the sample weight on the acceleration signal

In this second test series, we assessed the influence of the sample weight on the acceleration patterns during grinding of silica sand or iron ore. For each of these materials, we carried out five tests, increasing the sample load from 50 g to 90 g in steps of 10 g. Each run was carried out under identical conditions using the HSM 100P with a grinding time of 30 s and a rotation speed of 1200 rpm.

For silica sand, we found a characteristic change in the acceleration signal over time. In each run, the signal showed an initial uniform acceleration pattern without major fluctuations followed by an abrupt change to a pattern displaying an increasing fluctuation concomitant with a lowering of the absolute RMS values (Figure 3). The time of the signal change depended clearly on the sample weight, being systematically delayed with each increased sample load. Thus for 50 g, the signal change appeared at 9 s. For 60, 70, 80 and 90 g the change took place later at 15 s, 26 s, 28 s and 31 s, respectively (red arrows in Figure 3). The initial RMS values were similar between trials. In the run with 60 g of silica sand, the mean RMS before the signal change was 49.4 ± 1.8 $m s^{-2}$, thereafter 32.5 ± 8.5 $m s^{-2}$.

For iron ore, we observed a similar signal behaviour as for silica sand

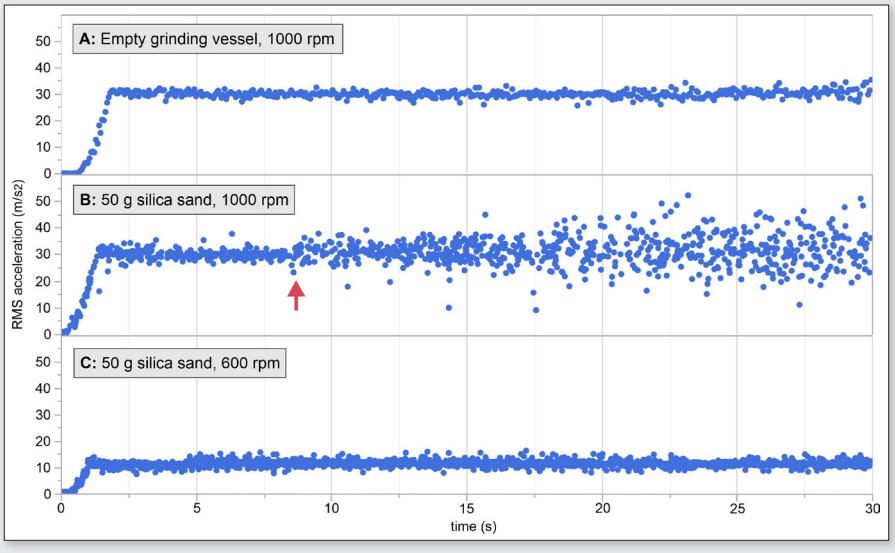

Figure 2. Monitoring RMS acceleration signals of an empty grinding vessel (A) and during efficient grinding (B) vs inefficient grinding (C) of pure silica sand.

(Figure 4). The time point of the signal change depended on the sample weight and increased from 12.5 s (50 g) to 25 s (90 g). However, the signal changes were smaller than for silica sand. For 60 g of iron ore, the mean RMS before the signal change was $50.1 \pm 2.6\,m\,s^{-2}$, thereafter $46.6 \pm 3.4\,m\,s^{-2}$.

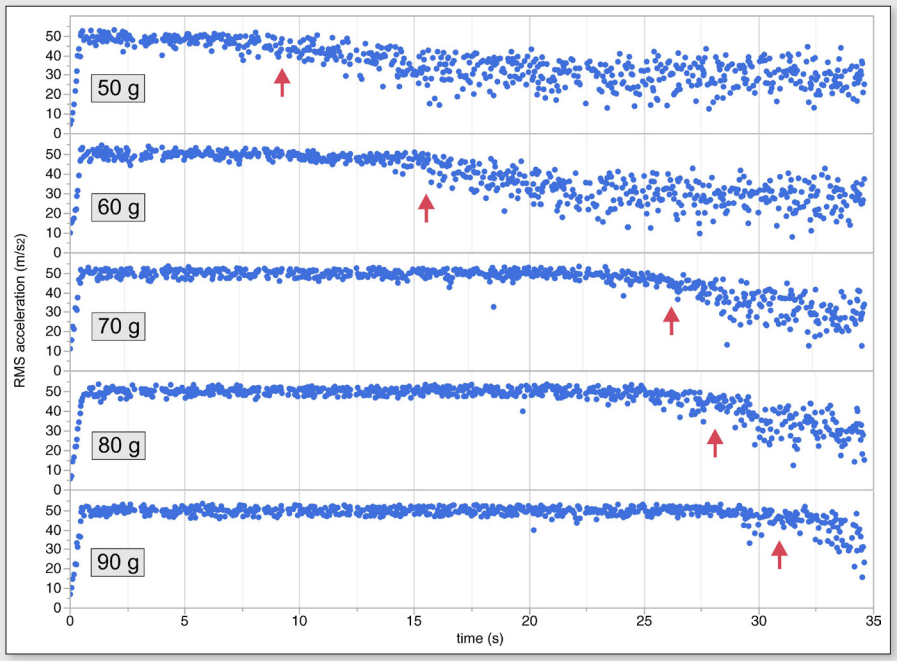

Figure 3. RMS acceleration signal assessed during grinding of different loads of silica sand in the manual disc mill of the type HSM 100P. The onset of the efficient grinding phase is characterised by an increase of the RMS variability (red arrow). The point of time when the signal changes depends on the sample weight.

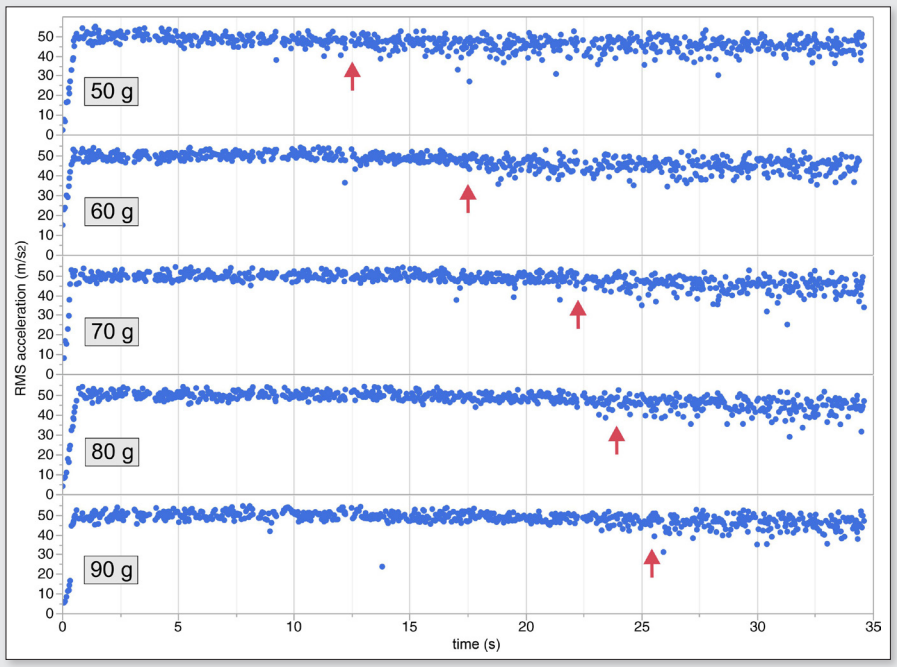

Figure 4. RMS acceleration signal assessed during grinding of different loads of iron ore in the manual disc mill (HSM 100P). Similar to results for silica sand, the onset of the efficient grinding phase is characterised by an increase of the RMS variability (red arrow). Also, here, the onset of the signal changes depends on the sample weight, but compared to silica sand, the iron RMS changes are less pronounced.

Influence of the rotation speed on acceleration signal and grain size distribution

In this test series, we examined the influence of different rotation speeds on the acceleration signal. The test runs were carried out on the semi-automatic HP-M 500 during grinding of 200 g of iron ore for 60 s. The rotation speed was different in each run (900, 1000, 1100 rpm). After each run, we determined the grain size distribution of the ground material using a vibratory sieve shaker.

For 900 rpm, the signal change occurred very late during the grinding process, at 57 s. For 1000 and 1100 rpm, the signal change was earlier, at 50 s and 38 s, respectively (Figure 5).

For the grain size analyses, we found an increase of the fraction < 45 µm from 41.2 % at 900 rpm to 51.0 % at 1000 rpm and 59.6 % at 1100 rpm. At the same time, the fraction > 150 µm decreased from 31.2 % to 17.3 % and 6.4 %, respectively (Figure 6).

Oscillation analysis

In order to evaluate the underlying cause for the change of the acceleration signal during grinding we performed an oscillation analysis. We examined the RMS signal during grinding of iron ore in an automatic mill (HP-MP) at a rotation speed of 1000 rpm. For all the tests above we initially observed a uniform signal with little fluctuation which then changed to a signal with larger fluctuations (Figure 7). In order to try to understand more, we performed an oscillation analysis *before* the signal change (red box at 10 s, Figure 7) and later (red box at 15 s, Figure 7).

For this purpose, the acceleration values in the x- and y-direction on an ideal sinusoidal oscillation were projected on a graph (Figure 8). When set in motion, the grinding vessel describes a circular path around its centre. Therefore, the acceleration in the x- and y-direction shows a phase lag of 90° in Figure 8.

At 10 s the values for x- and y-acceleration are located on the ideal reference sinusoidal curves (Figure 8A). Also, the phase lag of x- and y-acceleration was quite constant at 90°. Accordingly, the resulting RMS values of x- and y- direction plot in a relatively straight line with very little deviation. This corresponds to a situation when the grinding vessel can move relatively undisturbed along its ideal circular path. After 15 s we found that some of the x- and y-acceleration values were lower than

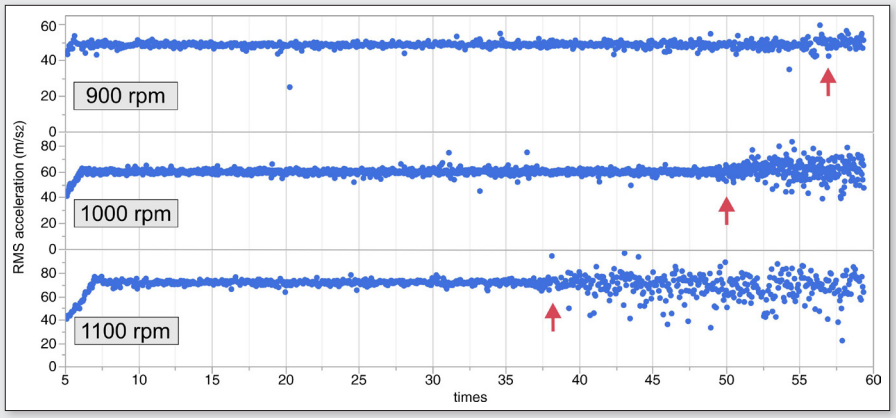

Figure 5. RMS acceleration signal representing grinding of 200 g iron within the HP-M 500. The rotation speed varied from 900 rpm to 1000 rpm. The grinding time in all trials was 60 s. The onset of the signal change (red arrow) depend on the rotation speed with earlier starts at higher rpm values.

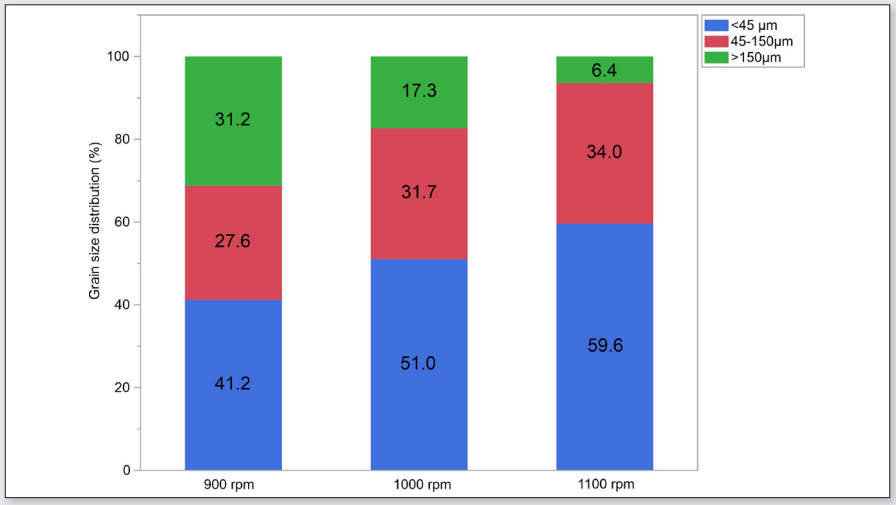

Figure 6. Empirical grain size distribution after grinding of 200 g iron ore in the HP-M 500 at different rotation speeds for 60 s.

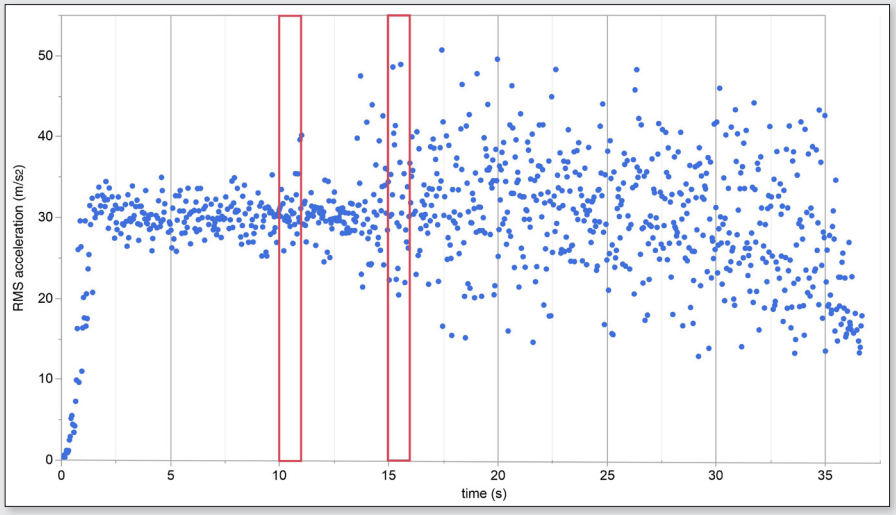

Figure 7. RMS acceleration signal during grinding of 60 g iron ore in an automatic mill (combined mill and press of the type HP-MP). The recording was used to guide an oscillation analysis at two different times each covering 1 s (red boxes). The first oscillation analysis was carried out before increase of the acceleration variability (at 10 s), and the second analysis after the transition to efficient grinding had occurred (at 15 s).

predicted by the ideal sinusoidal curve (Figure 7B). These temporary decelerations are interpreted to be the cause of the increased variability of the RMS signals in this test.

Discussion

In this study, we introduce a new method for real-time monitoring of the grinding efficiency in disc mills. We demonstrate that the increase in acceleration variability, and the concomitant decrease of acceleration magnitude, is a suitable *proxy marker* for efficient grinding. This finding is corroborated by the following observations: 1) Motion of an empty grinding vessel produced only a uniform acceleration signal with low variability. 2) Inefficient grinding due to slow rotation speeds, or high sample load, is characterised by absence, or late onset of the characteristic increased acceleration variability. 3) By contrast, efficient grinding is correlated with an early and swift increase in acceleration variability. At the same time the mean acceleration magnitude is decreased.

The described signal patterns were observable in all disc mill types used in this study, including manual and automatic mills with a 100 cm^3 tungsten carbide grinding vessel as well as a semi-automatic mill with a 500 cm^3 chrome steel vessel. This shows that the signal pattern is a *general phenomenon* that likely can be utilised for a wide range of different discs mills and applications.

The underlying reason for the characteristic signal pattern change is not yet fully understood. The first oscillation analysis showed that increased variability is attributable to brief *decelerations* of the grinding vessel in the x- or y-directions. We believe that these acceleration interruptions are due to short blockages of the motion of the grinding set (puck and ring). The impeded motion of the grinding set likely leads to momentary decelerations of the entire grinding vessel which can be measured by the acceleration sensor.

What is the reason for increased motion blockage of the grinding set within the vessel during efficient grinding? The flowability and "effective viscosity" of powders strongly depends on the particle size and shape.[5,6] At small average particle sizes and, therefore, high inter-particular forces, stable bridges are formed between particles. Moreover, these bridges are not only stable but also reform quickly. At the beginning of the grinding process, the average particle size is large and hardly any inter-particular bridges are built. This means that flowability

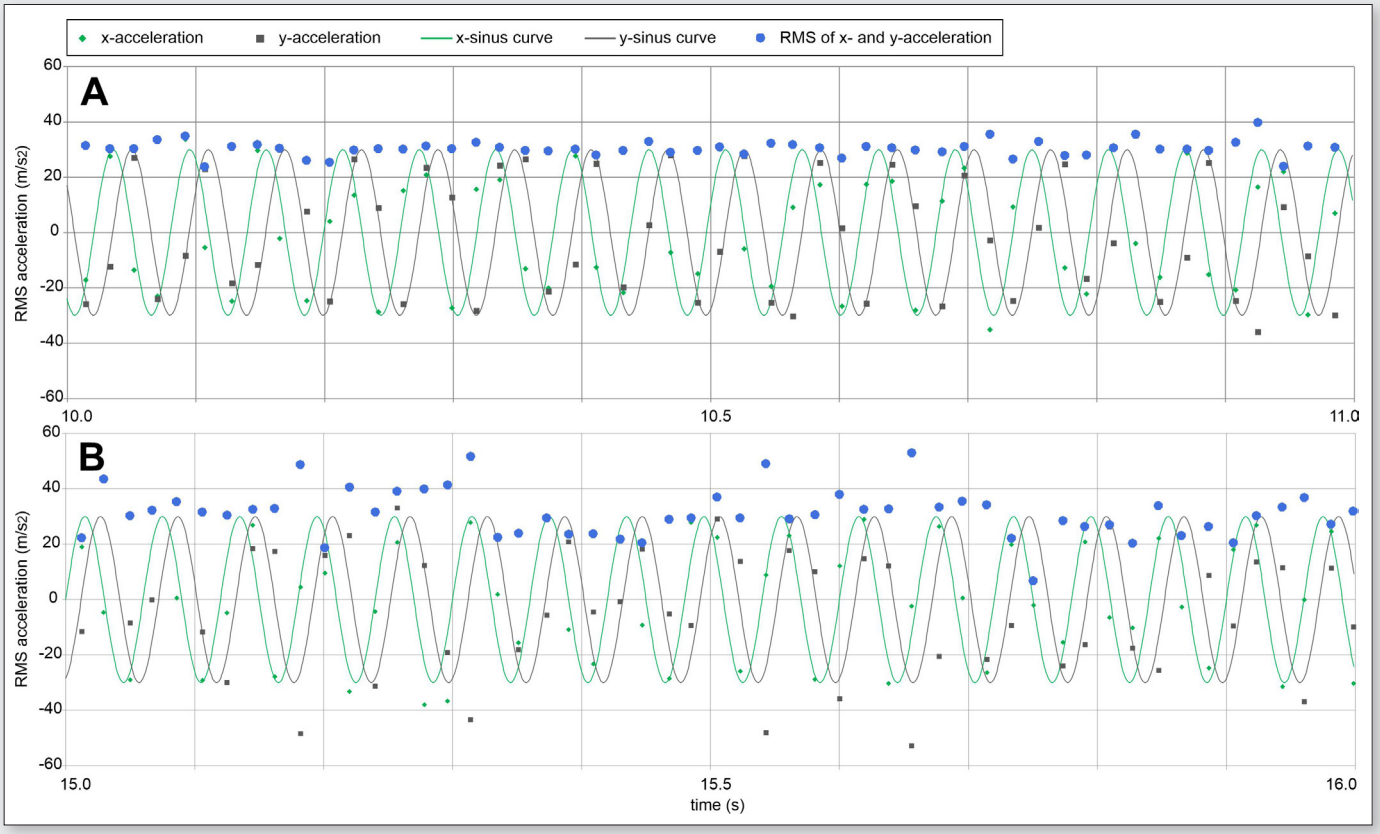

Figure 8. Oscillation analysis of the grinding run shown in Figure 6 for two different time points—*before* onset of variability increase at 10 s (A) and *after* increase at 15 s (B). If the grinding vessel shows a completely undisturbed circular motion, the x- and y-accelerations can be described as sinusoidal curves with a phase lag of 90° (green and black curves). (A) Before onset of efficient grinding the measured x- and y-acceleration values plot along these curves resulting in constant RMS values. (B) After onset of efficient grinding, x- and y-values show significant decelerations with deviations from the ideal curve, resulting in a higher sum-total variability of RMS values.

of the sample is high and, vice versa, viscosity is low. Therefore, the grinding set can move relatively unhindered through the powder within the grinding vessel.

However, as efficient grinding begins to take place, gradually the average particle size decreases. This leads to a build-up of inter-particular bridges resulting in lower flowability and higher viscosity. This in turn causes increasing blockage of the grinding set as measured by the increased acceleration variability.

What is the reason for decreased acceleration amplitude during efficient grinding? The increased variability during efficient grinding is accompanied by a general decrease of the total acceleration magnitude. This phenomenon *may* be due to transfer of the rotationally inducted kinetic energy into energy used for comminution of the sample material.

Conclusion

The accelerometer PAT monitoring approach opens up numerous opportunities for easy, real-time monitoring of the general grinding process. This is a smart-industry solution offering significant benefits in application development and condition monitoring of routine processes and samples. Basic models linking particle size distribution and sensory data from the grinding process can be used to define a Statistical Process Control (SPC) setup for automated sample preparation processes. Biasing factors, e.g. changes in material composition or preparation equipment wear, can be detected and appropriate counter-measures can be invoked.

Figure 9 shows a principal example of how such proxy observations can be used to develop calibration models for specific sample types. In Figure 9A a typical three-phase particle breakage evolution of multiple samples is captured, which can be linked to a certain Particle Size Distribution (PSD). This could be, for example, the calibration standards for an XRF instrument. The particle evolution itself is characterised by an initial phase where most of the bigger brittle particles are reduced in size (blue bar), followed by a second phase with a decreased size reduction efficiency (yellow bar). The third phase (red bar) is characterised by analytical precision disturbing agglomeration effects of the material.

In this example, a PSD of 80.7 % (±1.2 %) below 45 µm is expected for a reference or calibration sample after grinding. Therefore, this model can be used to evaluate the match of routine samples and gives an illustration of how a particular sample matches the expected procedural outcome. Thus, Figure 9B illustrates a sample plot within the calibrated model boundaries, while the sample shown in Figure 9C is clearly out of model range. Depending on the overall application scenario, this can, for example, indicate offsets in the preparation procedure, changes in raw material feed or in sample composition (e.g. mineral composition).The present experimental results show that high-resolution accelerometer sensor data would appear to be suitable to monitor automated processes in various ways. Here we are focusing on accelerometer sensor

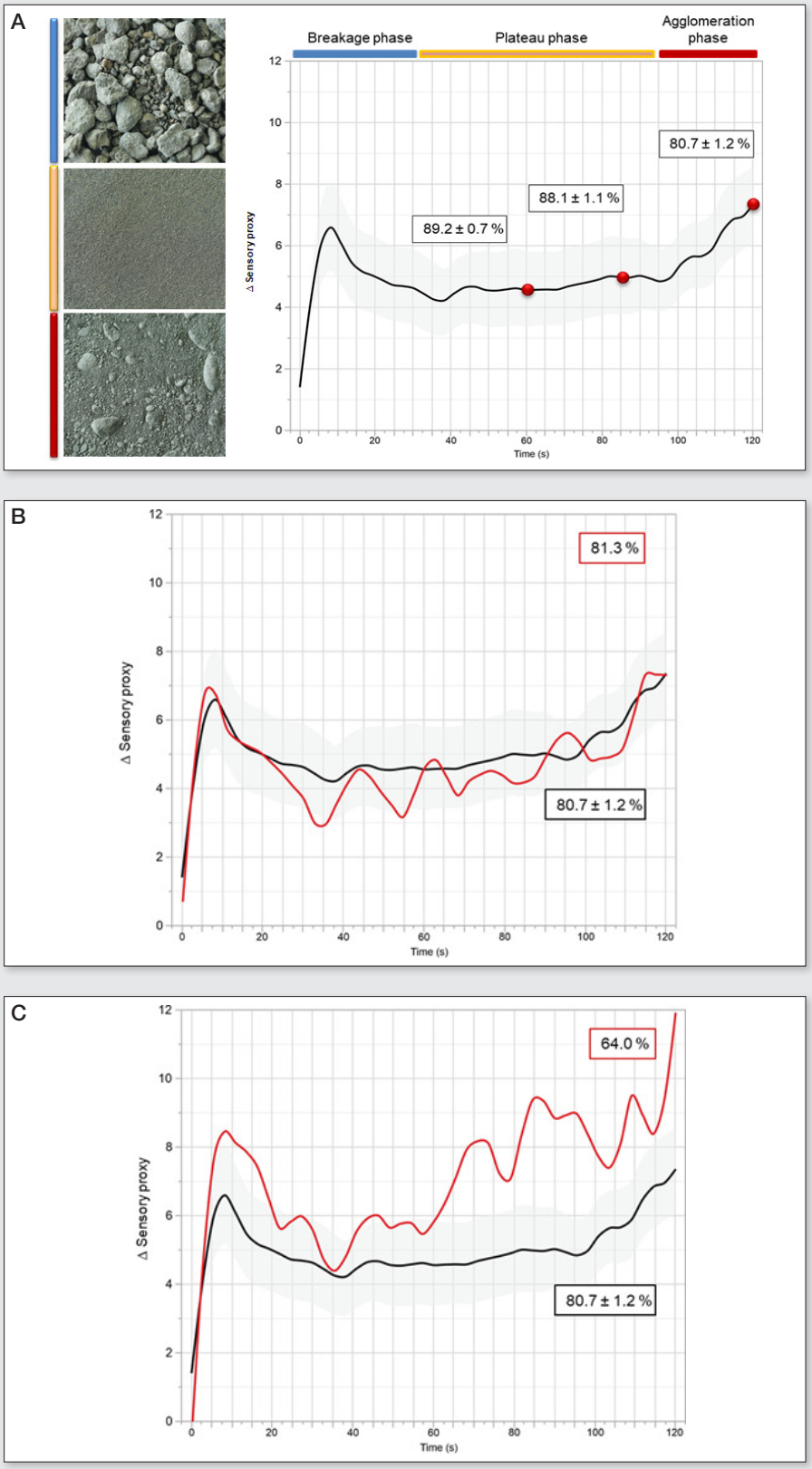

Figure 9. Schematic model for SPC of the grinding process in an automatic pulverising mill used to identify biasing changes in the measurement system caused by particle size effects. The bar far left shows a microscopic picture of the sample appearance according their comminution phase (see colour bar legend in A). A: Average sensor data model with specific PSDs to be expected (rel. values in boxes). The black line displays the mean of a set of calibration samples. Average particle size 80.7 % (±1.2 %) less than 45 µm. B: Routine sample with an acceptable range of expected PSD with 81.3 % less than 45 µm. C: Routine sample displaying an out of range PSD with 64.0 % less than 45 µm. Values in boxes: Relative content of particles below 45 µm.

types used for grinding sample preprocessing purposes. This type of approach also opens up the potential for powerful tool condition monitoring, analytical result validation and prediction of material changes in processes, all subject to further investigations on the nature and information content of observable PAT sensor data.

It is sometimes possible to augment the monitoring potential by also using complementary sensor types. This option, of course, strongly depends on the specific process a.o.[1]

References

1. K.A. Bakeev (Ed.), *Process Analytical Technology*, 2nd Edn. Wiley (2010). https://doi.org/10.1002/9780470689592
2. *Tool Condition Monitoring for Precise Evaluation of Milling Efficacy*. HERZOG Application note 19/2018. https://www.herzog-maschinenfabrik.de/medien/downloads/application-notes/?tx_news_pi1%5Bnews%5D=165&tx_news_pi1%5Bcontroller%5D=News&tx_news_pi1%5Baction%5D=detail&cHash=74499b1b32f353b36dbb98332744dd5d
3. Z. Mzyk, I. Baranowska and J. Mzyk, "Research on grain size effect in XRF analysis of pelletized samples", *X-Ray Spectrom.* **31,** 39–46 (2002). https://doi.org/10.1002/xrs.534
4. *Tool Condition Monitoring of Disc Mills—Monitoring of the Proper Swing Aggregate Function*. HERZOG Application note 25/2019. https://www.herzog-maschinenfabrik.de/medien/downloads/application-notes/?tx_news_pi1%5Bnews%5D=585&tx_news_pi1%5Bcontroller%5D=News&tx_news_pi1%5Baction%5D=detail&cHash=fbedf76ffe19e44b1f03a5aa58201ff2
5. *Tool Condition Monitoring of Disc Mills—Online Monitoring of the Wear of the Grinding Set*. HERZOG Application note 26/2019. https://www.herzog-maschinenfabrik.de/medien/downloads/application-notes/?tx_news_pi1%5Bnews%5D=588&tx_news_pi1%5Bcontroller%5D=News&tx_news_pi1%5Baction%5D=detail&cHash=be5ab495493b53b0c77222ebb7643610
6. J. Weigand, "Viscosity measurement on powders with a new viscometer", *Appl. Rheol.* **9(5),** 204–211 (1999). https://doi.org/10.1515/arh-2009-0014
7. T. Hao, "Analogous viscosity equations of granular powders based on Eyring's rate process theory and free volume concept", *RSC Advances* **5(115),** 95318–95333 (2015). https://doi.org/10.1039/C5RA16706J